Supporting Information for

Superior lithium-storage properties derived from a high pseudocapacitance behavior for a peony-like holey Co_3O_4 anode

Huanhuan Duan,[ab] Li Du,[ab] Shenkui Zhang,[ab] Zhuowen Chen,[ab] and Songping Wu*[ab]

a- School of Chemistry and Chemical Engineering, South China University of Technology, Guangzhou, 510641, China.

b- Guangdong Key Laboratory of Fuel Cell Technology, Guangzhou, 510641, China.

*Corresponding author, E-mail: chwsp@scut.edu.cn

Experimental section:

High and low temperature electrochemical performances were tested in a voltage range from 0.01-3.0 V with a digital-controlled oven (80 °C, Keelrein, Shanghai, China) and a refrigerator (-25 °C, SIEMENS, Germany), respectively.

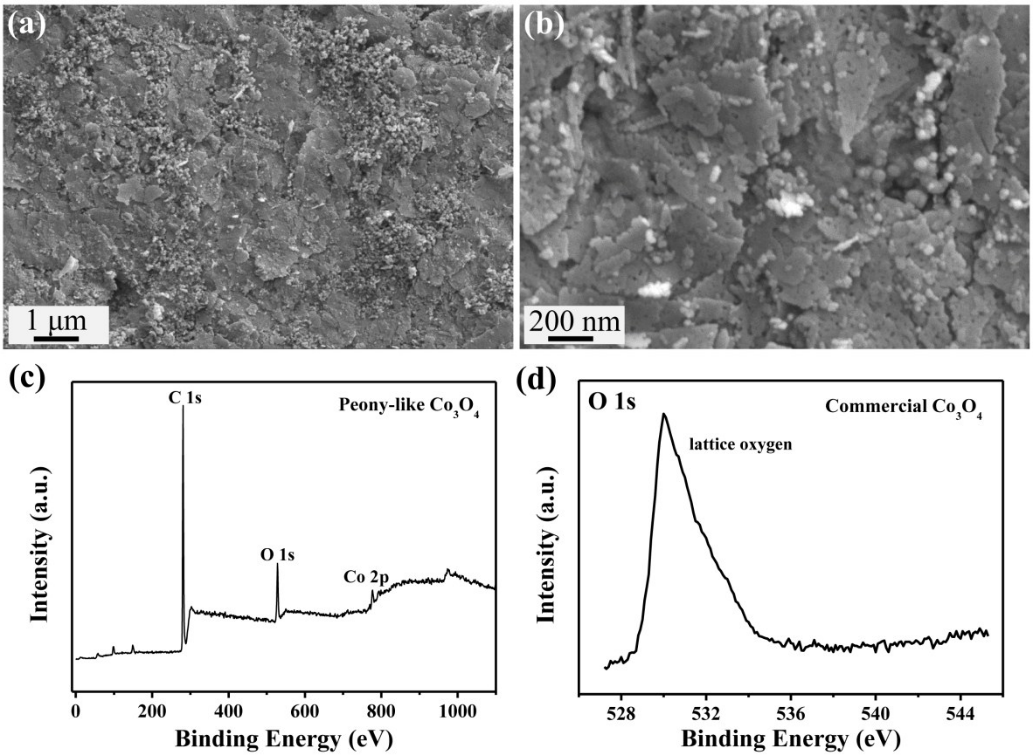

Figure S1. (a, b) SEM images of peony-like Co_3O_4 electrode after calendaring; (c) XPS survey spectrum of peony-like Co_3O_4; (d) O 1s XPS spectrum of commercial Co_3O_4.

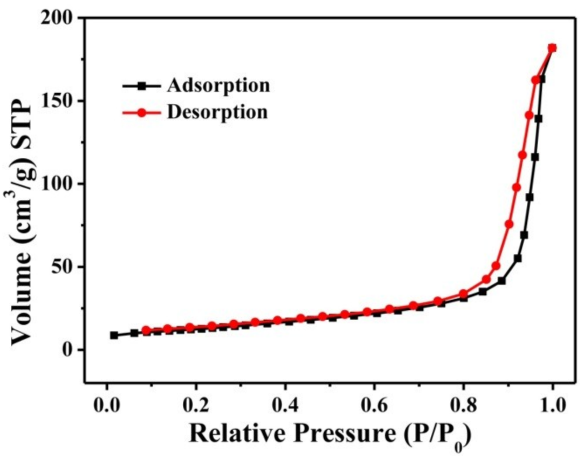

Figure S2. The nitrogen adsorption-desorption isotherms of Co_3O_4.

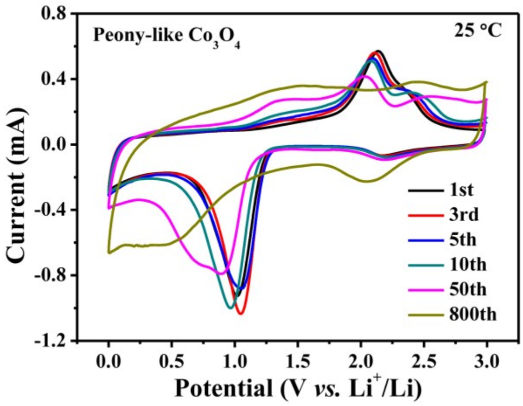

Figure S3. Cyclic voltammetry curves of peony-like Co_3O_4 at a scan rate of 0.5 mV s^{-1} with a current density of 500 mA g^{-1} after different cycles.

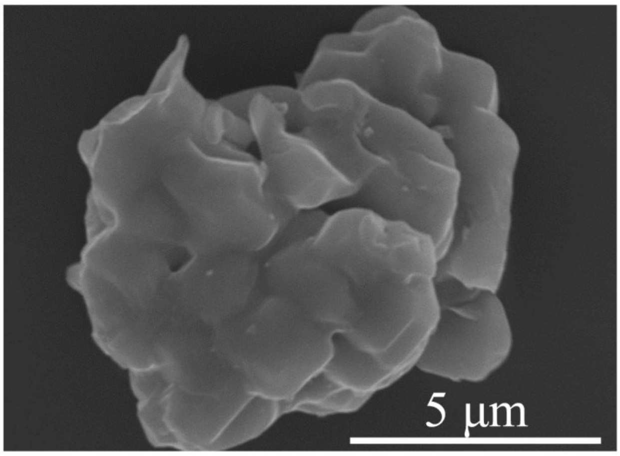

Figure S4. SEM image of commercial Co_3O_4 material.

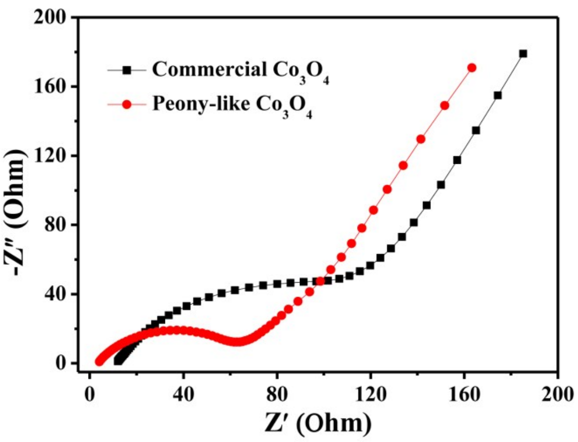

Figure S5. EIS profiles of peony-like Co_3O_4 and commercial Co_3O_4 electrode.

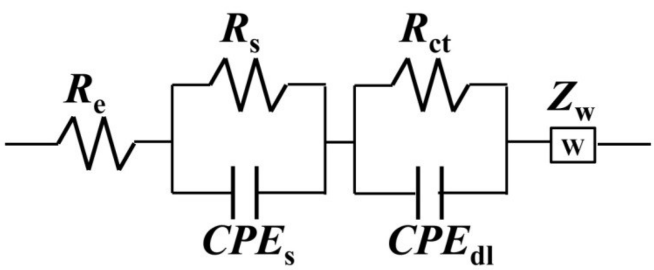

Figure S6. The equivalent circuit diagram of simulating peony-like Co_3O_4 and commercial Co_3O_4 electrodes assembled in coin cells. (R_e is electrolyte resistance, R_s is SEI layer resistance, R_{ct} is charge transfer resistance, CPE_s is surface films capacitance, CPE_{dl} is double-layer capacitance, Z_w is Warburg impedance.)

Table S1. Fitted kinetic parameters of peony-like Co_3O_4 and commercial Co_3O_4 electrodes, respectively.

Sample	R_e(Ω)	R_s(Ω)	R_{ct}(Ω)
Peony-like Co_3O_4 electrode	4.40	5.90	61.02
Commercial Co_3O_4 electrode	4.84	5.86	118.23

Table S2. Fitted kinetic parameters of peony-like Co_3O_4 electrode at a current density of 500 mA g^{-1} after different cycles.

Cycle Number	1st	3rd	5th	10th	50th	800th
$R_e(\Omega)$	4.40	4.39	4.80	4.5	5.01	15.23
$R_s(\Omega)$	5.90	5.43	4.32	5.11	5.35	5.50
$R_{ct}(\Omega)$	61.02	43.21	44.72	45.76	45.31	27.21

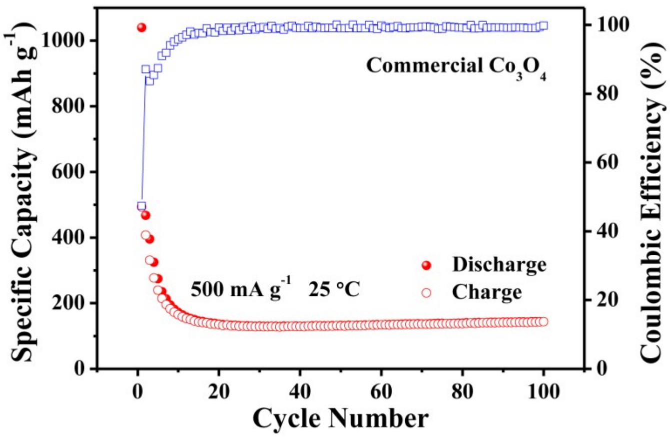

Figure S7. Cycle performance of commercial Co_3O_4 electrode at a current density of 500 mA g^{-1}.

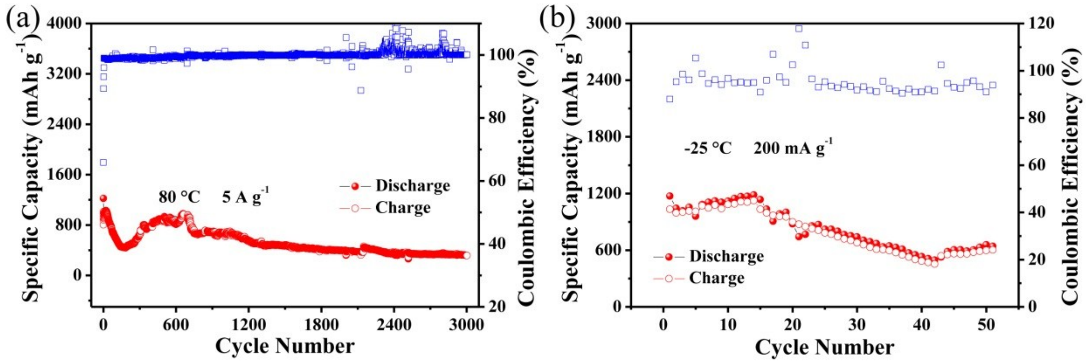

Figure S8. Electrochemical performances of peony-like Co_3O_4 at (a) 80 °C (@1 A g^{-1}); (b) -25 °C (@200 m A g^{-1}).

The results of high-temperature lithium-storage capability of peony-like Co_3O_4 electrode were shown in **Figure S8a**. The peony-like Co_3O_4 electrode achieved a first discharge capacity of 1220.9 mA h g^{-1} at a current density of 5.0 A g^{-1} under 80 °C, with an initial Coulombic efficiency of 65.9%. After 3000 cycles, a stable reversible capacity of 315.5 mA h g^{-1} was retained, which showed that this peony-like Co_3O_4 electrode possessed a good cycling stability under high temperature at a large current density. In addition, we also attempted to check the feasibility of as-prepared material as electrode under low temperature (-25 °C). As shown in **Figure S8b**, it is necessary to point out that the electrode rendered an initial discharge capacity of 1173 mA h g^{-1} at a current density of 200 mA g^{-1}, with a high Coulombic efficiency of 87%. After running 50 cycles, this electrode delivered a reversible capacity of 642 mA h g^{-1} with an average Coulombic efficiency of 95%, which can be ascribed to slow ion diffusion under low temperature.

Table S3. Electrochemical performances and physical parameters of cobalt oxide-based anode materials.

Morphology	**Synthesis method**	**Current rate (mA g^{-1})**	**Tempe - raptur e (°C)**	**Cycle number**	**Capacity (mAh g^{-1})**	**Ref.**
Hierarchical CNT/Co_3O_4 microtubes	chemical transformation/ annealing	1000 4000	25	200	782 577	1
Co_3O_4 hexagonal plates	solvothermal method	350	25	50	671 Co_3O_4-EtOH 485 Co_3O_4-MeOH 350 Co_3O_4-IPA 829 Co_3O_4-TT	2
Co_3O_4 hollow spheres	solution-based method	1000	25	100	1058	3
Hollow	Electrodepositi	500	25	100	1048	4

Co_3O_4/carb-on nanosheet composites	on/annealing					
Co_3O_4 hollow sphere	solvothermal method	1000 5000 5000	25	500 6000	924 335 219	5
Shale-like Co_3O_4	annealing	200	25	100	1045.3	6
Carbon-doped Co_3O_4 hollow nanofibers	electrospinning technique/hydrothermal method	200	25	100	1121	7
Co_3O_4 nanosheets	hydrothermal reactions/heat treatment process	200	25	100	1029	8
Bowknot-like Co_3O_4	hydrothermal method/ calcination	178 178 1780	25	1 100 500	1427.9 1388.8 751.3	9
N-doped 3D mesoporous Co_3O_4 network	dipping process/annealing	200 5000	25	200 700	957 485	10
Co_3O_4/Ag composite	dealloying method	1000	25	1000	468.5	11
Two-dimensional holey Co_3O_4 nanosheets	template-directed strategy	1000	25	200	850	12
Peony-like holey Co_3O_4	solvothermal method	**500** **10000** 5000	**25** **25** 80	**800** **1000** 3000	**1880** **341.4** 315.5	This work

	200	**-25**	**50**	**642**	

Table S4. The percentages of capacitive-effect contribution under different temperatures (-25, 25, 80 °C) with a series of sweep rates of 0.1, 0.3, 0.5, 1.0, 1.5 mV s^{-1}, respectively.

v **/mV s^{-1}** / **T/°C**	**0.1**	**0.3**	**0.5**	**1.0**	**1.5**
-25	25.0%	30.1%	36.0%	50.7%	57.2%
25	54.5%	63.2%	68.7%	77.9%	83.5%
80	57.1%	66.6%	74.7%	84.0%	90.0%

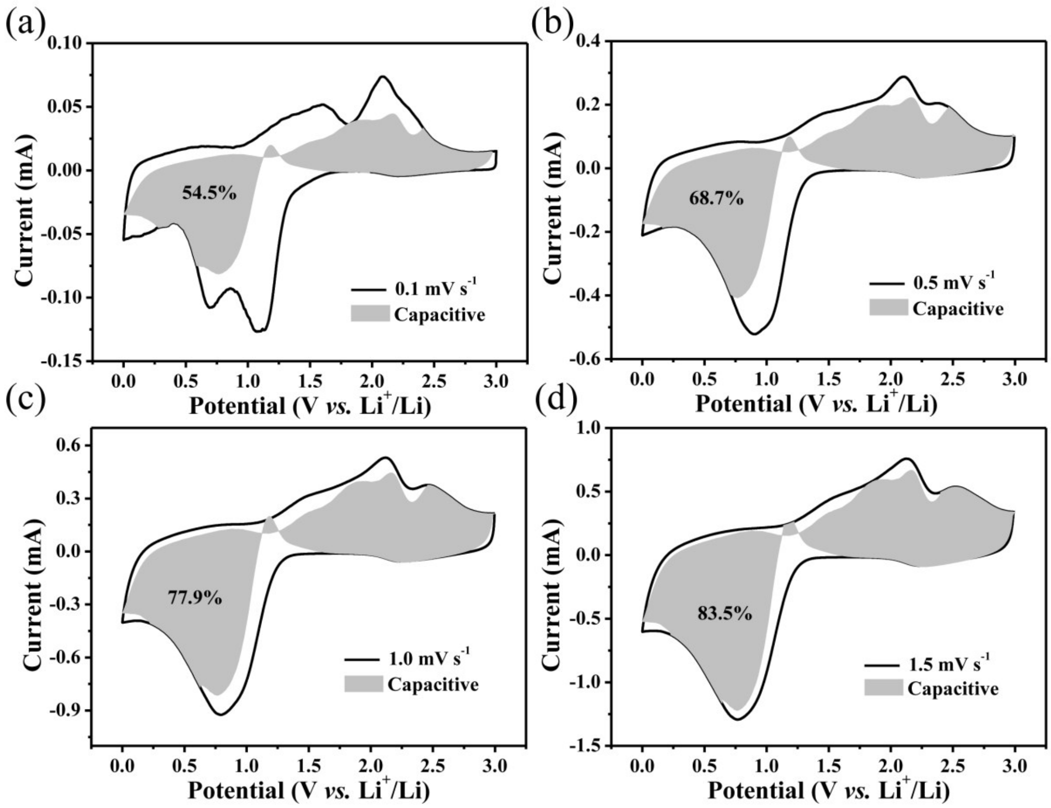

Figure S9. Capacitive contribution (shadow area) to total lithium-storage capacity at sweep rates of (a) 0.1 mV s^{-1}, (b) 0.5 mV s^{-1}, (c) 1.0 mV s^{-1}, (d) 1.5 mV s^{-1} under 25

°C.

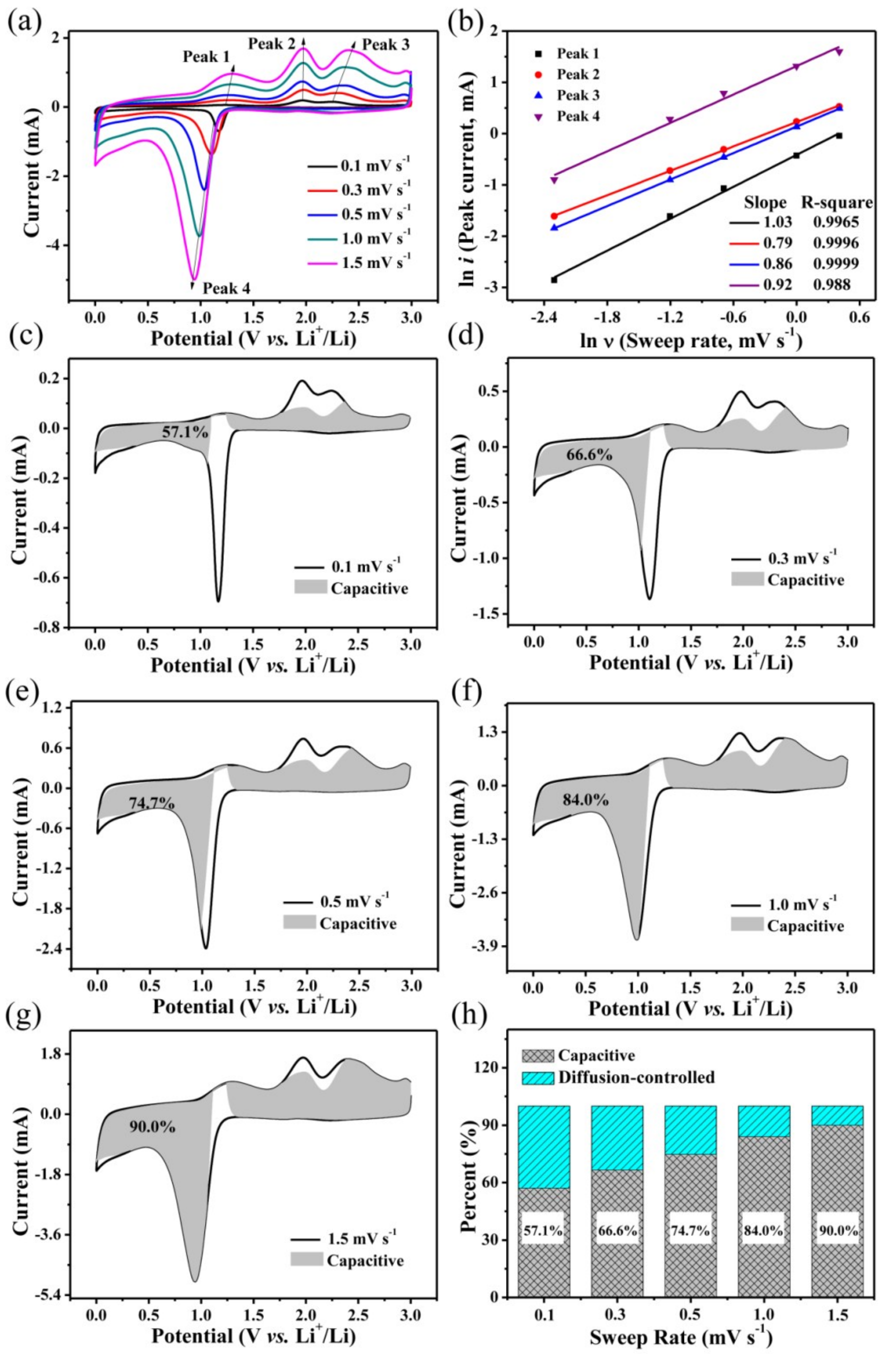

Figure S10. (a) CV curves after first three discharge/charge cycles with different sweep rates at 80 °C; (b) ln(*i*, peak current) versus ln(*v*, sweep rate) of four peaks (marked as 1-4 in (a)), and where fitted-line slope is b-value (There is a perfect fitting degree due to the value of R-square is close to ~1.); Capacitive contribution (shadow area) to total lithium-storage capacity at sweep rates of (c) 0.1 mV s^{-1}, (d) 0.3 mV s^{-1},

(e) 0.5 mV s^{-1}, (f) 1.0 mV s^{-1}, (g) 1.5 mV s^{-1}; (h) The percentages of capacitive-effect contribution at different sweep rates of 0.1, 0.3, 0.5, 1.0, and 1.5 mV s^{-1}.

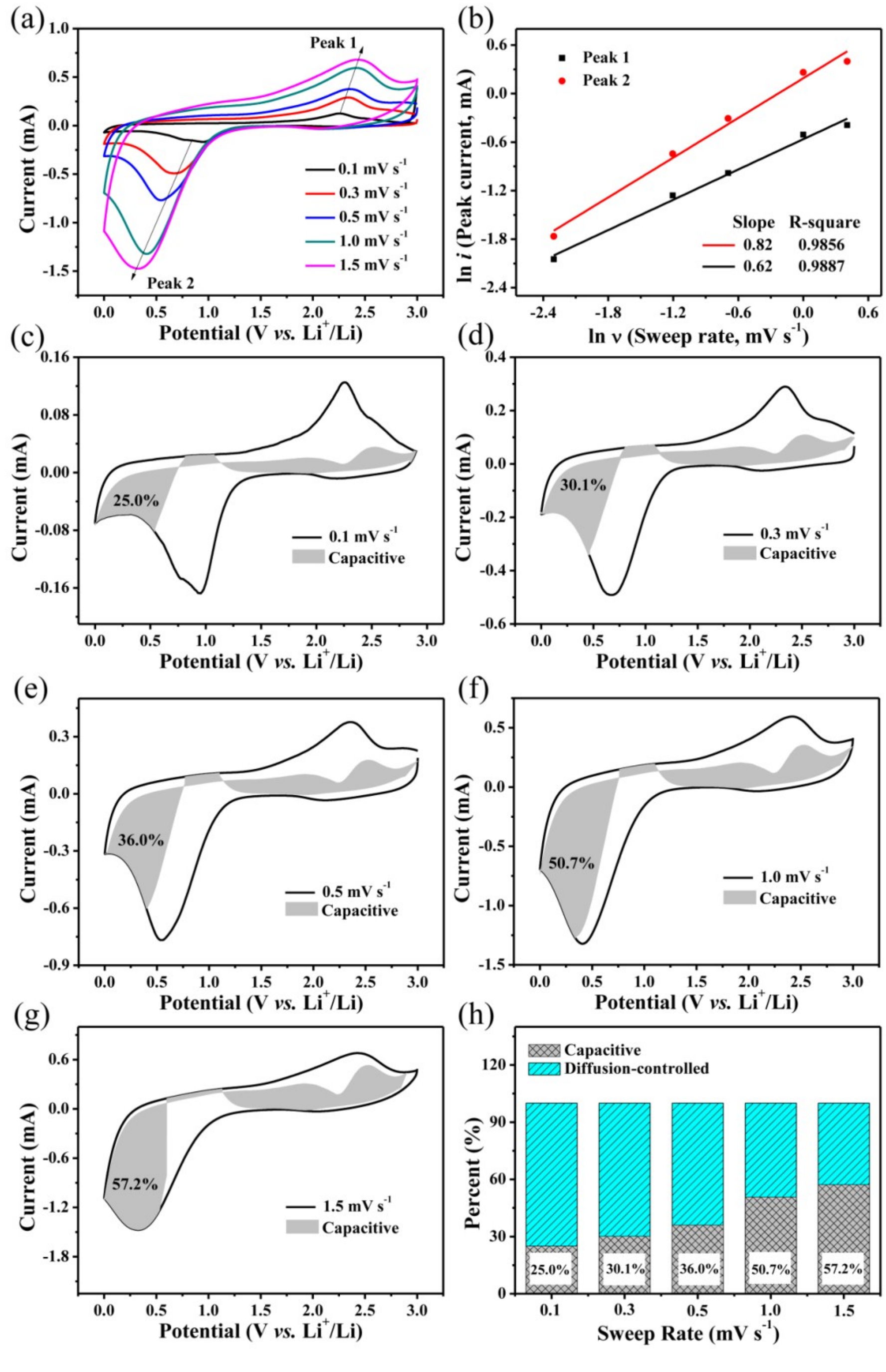

Figure S11. (a) CV curves after first three discharge/charge cycles with different sweep rates at -25 °C; (b) ln(i, peak current) versus ln(v, sweep rate) of two peaks (marked as 1-2 in (a)), and where fitted-line slope is b-value (There is a perfect fitting degree due to the value of R-square is close to ~1.); Capacitive contribution (shadow area) to total lithium-storage capacity at sweep rates of (c) 0.1 mV s^{-1}, (d) 0.3 mV s^{-1}, (e) 0.5 mV s^{-1}, (f) 1.0 mV s^{-1}, (g) 1.5 mV s^{-1}; (h) The percentages of capacitive-effect contribution at different sweep rates of 0.1, 0.3, 0.5, 1.0, and 1.5 mV s^{-1}.

References:

1 Y. M. Chen, L. Yu and X. W. Lou, *Angew. Chem. Int. Ed.*, 2016, **55**, 5990-5993.

2 W. Zhao, X. Zhou, I. J. Kim and S. Kim, *Nanoscale*, 2017, **9**, 940-946.

3 J. Z. Yin, Y. Zhang, Q. Y. Lu, X. L. Wu, Z. J. Jiang, L. Y. Dang, H. F. Ma, Y. Y. Guo, F. Gao and Q. Y. Yan, *J. Mater. Chem. A*, 2017, **5**, 12757-12761.

4 L. Peng, Y. Y. Feng, Y. J. Bai, H. J. Qiu and Y. Wang, *J. Mater. Chem. A*, 2015, **3**, 8825-8831.

5 H. Sun, G. Xin, T. Hu, M. Yu, D. Shao, X. Sun and J. Lian, *Nat. Commun.*, 2014, **5**, 4526.

6 H. H. Li, Z. Y. Li, X. L. Wu, L. L. Zhang, C. Y. Fan, H. F. Wang, X. Y. Li, K. Wang, H. Z. Sun and J. P. Zhang, *J. Mater. Chem. A*, 2016, **4**, 8242-8248.

7 G. C. Chunshuang Yan , Xin Zhou , Jingxue Sun , and Chade Lv, *Adv. Funct. Mater.*, 2016, **26**, 1428-1436.

8 D. Zhang, W. Sun, Z. Chen, Y. Zhang, W. Luo, Y. Jiang and S. X. Dou, *Chemistry*, 2016, **22**, 18060-18065.

9 H. R. Du, C. Yuan, K. F. Huang, W. H. Wang, K. Zhang and B. Y. Geng, *J. Mater. Chem. A*, 2017, **5**, 5342-5350.

10 S. Zhu, J. J. Li, X. Y. Deng, C. N. He, E. Z. Liu, F. He, C. S. Shi and N. Q. Zhao, *Adv. Funct. Mater.*, 2017, **27**, 1605017.

11 Q. Hao, Y. Yu, D. Y. Zhao and C. X. Xu, *J. Mater. Chem. A*, 2015, **3**, 15944-15950.

12 D. H. Chen, L. L. Peng, Y. F. Yuan, Y. Zhu, Z. W. Fang, C. S. Yan, G. Chen, R. Shahbazian-Yassar, J. Lu, K. Amine and G. H. Yu, *Nano Lett.*, 2017, **17**, 3907-3913.